AUT Journal of Electrical Engineering
10.22060/EEJ.2026.25375.5921

Regularization-Structured Autoencoder for Enhanced Deep Learning-Based Indoor Localization in Complex Wireless Environments

Ali Karimi[1] and Meysam Raees Danaee[2*]

[1] Phd Candidate, Faculty of Electrical Engineering, Imam Hossein University, Tehran, Iran
[2] Faculty of Electrical Engineering, Imam Hossein University, Tehran, Iran

Abstract:

Indoor localization is a key enabler of smart environments, yet achieving high-accuracy positioning remains difficult due to severe multipath effects, signal distortion, and the limited ability of current deep models to generalize across heterogeneous wireless datasets. Most existing approaches overlook the intrinsic sparsity structure of wireless signal features, leading to unstable latent representations and reduced robustness in complex indoor scenarios. To bridge this gap, this paper proposes a non-smooth regularized autoencoder that embeds a sparsity-inducing non-smooth regularizer into the latent space, enabling the extraction of compact, noise-resilient, and interpretable spatial features from high-dimensional signal measurements. This design introduces a clear advancement over state-of-the-art autoencoder and regression-based models, which predominantly rely on smooth penalties and consequently struggle under strong non line of sight conditions. Evaluations on the UJIIndoorLoc benchmark show that the non-smooth regularized autoencoder achieves an average localization error of 6.78 m, outperforming conventional deep neural network baselines. Furthermore, experiments on a real-world CSI dataset collected in a 13.5×11 m² cluttered laboratory demonstrate a mean error of 1.73 m in a challenging non line of sight environment. These findings confirm that the proposed non-smooth regularized autoencoder effectively addresses core challenges in robust feature learning and offers strong generalization across diverse indoor settings, establishing it as a powerful framework for next-generation indoor localization systems.

Keywords:

Deep neural network, indoor localization, autoencoder, non-smooth regularization.

10.22060/EEJ.2026.25375.5921

* Corresponding author's email: mraeesdanaee@ihu.ac.ir

1. Introduction

With the rapid growth of Internet of Things (IoT) applications and the increasing demand for location-based services, accurate indoor localization has become a critical challenge in wireless communications and machine learning research. While global positioning systems (GPS) perform well in outdoor environments, their accuracy dramatically decreases in indoor environments due to obstacles, multipath effects, and signal attenuation. In this context, Wi-Fi-based indoor localization has emerged as a practical solution due to the widespread availability of Access Points (APs) and low deployment cost.

Traditional indoor localization methods rely mainly on triangulation, signal propagation models, or fingerprinting. Among these, fingerprinting has gained the most attention due to its ability to adapt to different environments without detailed channel modeling. However, fingerprinting is often dependent on high-dimensional and noisy data such as Received Signal Strength Indicator (RSSI) or Channel State Information (CSI), which are affected by environmental changes, multipath propagation, and device heterogeneity. Therefore, efficient feature extraction techniques for dimensionality reduction and discriminative representation of location data are crucial, because high-dimensional wireless measurements often contain redundant, noisy, and environment-dependent variations that can obscure meaningful spatial patterns and significantly degrade localization accuracy.

Recent deep learning-based localization systems leverage large-scale datasets to learn hierarchical feature representations that effectively characterize wireless signals. Owing to their multi-layer architecture, deep neural networks can efficiently process high-dimensional data and capture complex spatial relationships embedded in the signal measurements. Furthermore, these models not only perform robust feature extraction but also directly estimate user positions with high precision, thereby improving localization accuracy and robustness while reducing the adverse effects of noise, multipath propagation, and dynamic environmental variations.

10.22060/EEJ.2026.25375.5921

For instance, the work in [1] proposed a deep learning based indoor localization system by semi-supervised localization algorithm that mitigates prediction bias by modeling non-stationary data distributions instead of relying on a fixed Gaussian assumption. Employing a transformer-based architecture, the framework captures long-range dependencies within RSSI measurements and augments the training set using pseudo-labeled samples with low uncertainty. Experimental outcomes demonstrated that this adaptive learning mechanism yields superior stability and accuracy compared to conventional supervised models, particularly in environments with limited labeled data and complex signal propagation conditions.

To address spatial complexity in multi-building environments, authors in [2] introduced a three-dimensional localization framework that performs hierarchical position estimation at building, floor, and coordinate levels. The approach initially reconstructs incomplete RSSI signals using recurrent environmental features and subsequently refines spatial inference across multiple scales. This hierarchical modeling strategy enhances positioning precision, reduces computational overhead and energy consumption, and increases robustness against noise and signal interference. The reported average localization error, remaining within a moderate spatial range, confirms the system's superior effectiveness compared to conventional fingerprinting approaches. Also, authors in [3], a WiFi-based localization model integrates transfer learning for domain-invariant feature extraction with deep reinforcement learning for dynamic adaptation to environmental variations, significantly reducing the dependence on labeled samples.

In the last years, research attention has increasingly shifted toward network model robustness and stability. Deep learning approaches, particularly Auto-Encoders (AEs), have opened new opportunities in this field [4-8]. Autoencoders, with their encoder–decoder architecture, can learn hidden representations and compact embeddings from complex input data. One notable approach employed stacked denoising autoencoders combined with data augmentation techniques to reduce sensitivity to noise and environmental variations, leading to more reliable localization [9].

In [10], the authors employed a Stacked AE (SAE) followed by a Fully Connected (FC) network for multi-building and multi-floor classification. They demonstrated that prior hierarchical processing approaches [11] incur high computational complexity, requiring careful feature selection and a separate classifier for each level (e.g., building first, then floor identification). The SAE serves primarily for dimensionality reduction, which is critical because Wi-Fi fingerprints must ideally encompass all detected APs in an environment; however, only a subset of APs is typically observed at different locations due to signal dropout. This issue is particularly pronounced in large-scale environments. The FC network then maps the compressed representation to its corresponding class, where each class represents a building-floor combination (e.g., the fourth floor of the second building). Their approach achieved a classification accuracy of 92% on the widely used UJIIndoorLoc dataset.

Building upon [10], Kim in [12] and [13] also utilized SAE for dimensionality reduction, followed by an FC network for hierarchical and multi-label classification. A weighted loss function was employed in the FC network to account for class imbalance. Their experiments were conducted on the UJIIndoorLoc dataset, which comprises 933 distinct rooms, corresponding to 933 output nodes for multi-class classification. To reduce network complexity, the authors proposed a novel strategy that effectively reduced the number of output nodes to 118. The evaluated results reported an average localization error of approximately 9.29 m, demonstrating the effectiveness of SAE-based dimensionality reduction in large-scale indoor positioning scenarios. Authors in [14] combined Convolutional Autoencoders (CAEs) with Convolutional Neural Networks (CNNs) to jointly perform dimensionality reduction and fine-grained spatial inference, achieving an average localization error of 9.5 m on the UJIIndoorLoc dataset. Although this and other recent deep learning-based localization methods have demonstrated promising performance, they remain vulnerable to overfitting and performance degradation when processing noisy or high-dimensional input data. Motivated by these challenges, the proposed method employs a non-smooth regularized deep autoencoder framework that effectively enhances feature representation, improves robustness against noise, and strengthens the generalization capability of the localization model, thereby providing more reliable and accurate indoor positioning in complex wireless environments.

In indoor localization research, the integration of autoencoders with specialized regularizations has been shown to significantly enhance feature discriminability and robustness. For example, sparse autoencoders with an activity penalty term have been used to denoise Wi-Fi RSSI fingerprints and significantly improve Wi-Fi fingerprint-based indoor localization accuracy [15]. Variational autoencoders (VAEs), which impose a probabilistic regularization via the KL-divergence, have been employed to extract generalizable spatial representations in localization tasks [16]. Moreover, semi-supervised frameworks combining autoencoders with Laplacian regularization have demonstrated that both labeled and unlabeled fingerprint data can be exploited effectively [17]. In [18], Kim and Lee proposed an adaptive Denoising Autoencoder (DAE) to improve RSSI-based indoor localization in Bluetooth Low Energy (BLE) environments. Instead of employing conventional Gaussian noise, the proposed method introduces an adaptive noise model that reflects the distance-dependent characteristics of RSSI measurements, enabling the network to learn more robust and discriminative feature representations. This regularization strategy effectively suppresses noise while preserving the intrinsic structure of RSSI fingerprints, resulting in improved localization accuracy and generalization. The experimental results demonstrate that adaptive feature regularization significantly enhances the robustness and reliability of fingerprint-based indoor positioning systems in complex wireless environments. Also, in [2], the authors propose a robust indoor localization framework based on regularized feature learning, where the learned representations are explicitly decomposed into environment-invariant and position-related features. This regularization strategy encourages the model to preserve stable and transferable characteristics of RSSI fingerprints while suppressing environment-specific variations and irrelevant noise, thereby improving the discriminative capability of the latent feature space. By jointly optimizing invariant and localization-sensitive representations, the proposed framework enhances generalization across different buildings and

10.22060/EEJ.2026.25375.5921

floors, reduces the impact of signal fluctuations and environmental dynamics, and ultimately achieves more reliable and accurate indoor localization performance in complex multi-building scenarios.

Also, combining sparse autoencoders with particle filters improved Wi-Fi localization accuracy in [19]. Specifically, sparse autoencoders, which apply non-smooth regularizers such as $\ell 1$-norm constraint, ensure that only a subset of neurons is active [20]. This mechanism guides the network to focus on the most important patterns while suppressing irrelevant features, because non-smooth regularizers such as $\ell 1$ impose sparsity in the latent space by penalizing small or noisy activations more aggressively than smooth penalties. As a result, uninformative components are driven toward zero, allowing the model to retain only salient propagation cues and yielding a more stable and discriminative representation for indoor localization systems. Recent studies such as [21] also highlight the significance of non-smooth regularization in feature learning. Non-smooth penalties, such as $\ell 1$, force the network to concentrate on the essential features and prevent overfitting, which is particularly important in high-dimensional, noisy fingerprint data.

Recently, graph-based deep learning has become a promising approach for Wi-Fi fingerprint-based indoor localization by modeling the structural relationships among fingerprint measurements. Li *et al.* [22] proposed HoGNNLoc, a high-order Graph Neural Network that exploits graph representations of Wi-Fi fingerprints to capture spatial correlations and improve localization robustness. Similarly, Kim *et al.* [23] introduced a Variational Graph Autoencoder (VGAE) framework that performs feature-level augmentation by modeling the relationships between reference points and access points, thereby improving localization accuracy under incomplete RSSI measurements. Despite their effectiveness, these methods rely on graph construction and message-passing operations, leading to higher computational complexity. In contrast, the proposed method employs a regularized deep autoencoder to learn compact and discriminative latent representations directly from fingerprint data without graph topology construction, resulting in a simpler and more computationally efficient framework while maintaining competitive localization performance.

Recently, self-supervised and contrastive learning have shown great potential for Wi-Fi fingerprint-based indoor localization by learning robust representations from unlabeled data. Rizk and Elmogy [24] proposed SelfLoc, which employs a self-supervised dual-contrastive learning strategy for robust feature representation, while Shen *et al.* [25] introduced VF-CLIP, integrating virtual feature maps with contrastive learning to improve localization robustness under dynamic environments. In contrast, the proposed method employs a regularized deep autoencoder to learn compact and discriminative latent representations directly from fingerprint data, providing a simpler and computationally efficient framework without requiring contrastive objectives or self-supervised pretext tasks.

Taken together, these findings indicate that deep autoencoders with non-smooth regularizers provide a promising research direction for indoor localization. This approach not only enhances positional accuracy but also improves model stability and generalization under dynamic environmental conditions. In this study, we propose a novel framework for single-user Wi-Fi localization that integrates autoencoders with non-smooth regularization and we evaluate its performance against conventional methods.

Recent advances in deep learning have substantially improved the performance of Wi-Fi fingerprint-based indoor localization through the development of increasingly sophisticated architectures, including deep autoencoders, graph neural networks, and self-supervised representation learning frameworks. While these approaches have achieved remarkable localization accuracy, most of them rely on complex network designs, additional feature extraction mechanisms, or large-scale annotated datasets, often resulting in increased computational complexity and reduced deployment efficiency. In contrast, the proposed framework demonstrates that significant performance improvements can be achieved without increasing architectural complexity. By integrating a non-smooth $\ell 1$ regularization strategy into a deep autoencoder, the proposed method learns more discriminative and sparse latent representations that are inherently more robust to measurement uncertainty and environmental variations, particularly under challenging NLOS conditions. Consequently, the proposed method provides an effective balance between localization

10.22060/EEJ.2026.25375.5921

accuracy, robustness, and computational efficiency, distinguishing it from recent deep learning-based indoor localization approaches that primarily pursue performance gains through increasingly complex network architectures.

The following sections of this paper are organized as follows. Section II offers a detailed overview of the system architecture, elaborating on the design of the proposed model and the structure of the indoor localization framework built upon a deep learning network equipped with an autoencoder incorporating non-smooth regularization terms. Section III introduces a dedicated analysis of non-smooth regularization mechanisms and their role in preventing overfitting in deep autoencoders. Section IV outlines the mathematical principles, optimization formulations, and evaluation criteria adopted throughout the study to ensure a rigorous analytical foundation. Section V presents an extensive set of numerical analyses and simulation experiments aimed at validating the effectiveness of the proposed model and verifying the accuracy of the derived formulations. The results presented in this section demonstrate the model's capability to reliably capture the complex structure of the data and provide robust localization performance under various conditions and heterogeneous datasets. Finally, Section VI concludes the paper by summarizing the findings and outlining potential directions for enhancing the accuracy of neural-network-based indoor localization systems.

2. The Proposed System Model

The proposed indoor localization system operates in two main stages: offline training and online position estimation. During the offline training phase, RSSI or CSI measurements are collected from multiple APs across different locations of the building. A deep learning network with a SAE architecture, incorporating non-smooth regularization techniques, is then trained to learn a low-dimensional representation of the RSSI or CSI data. Subsequently, a fingerprint database is constructed to store the mapping between the learned low-dimensional representations and their corresponding physical locations.

10.22060/EEJ.2026.25375.5921

In the online position estimation phase, RSSI or CSI data are measured at an unknown location. These measurements are passed through the pre-trained autoencoder to obtain their low-dimensional representation. This representation is then compared with entries in the fingerprint database using Euclidean distance to identify the closest match, thereby determining the estimated location. Given that Wi-Fi fingerprints are typically noisy and subject to temporal, environmental, and device-dependent variations, and considering that the communication links between many access points and the designated receiver may experience recurrent outages, the autoencoder serves as a powerful tool to denoise and extract meaningful features, thereby providing robust and reliable fingerprints for indoor localization.

An autoencoder consists of two coupled parametric mappings: an encoder and a decoder, which are jointly optimized to learn an efficient latent representation of the input data. Formally, the encoder

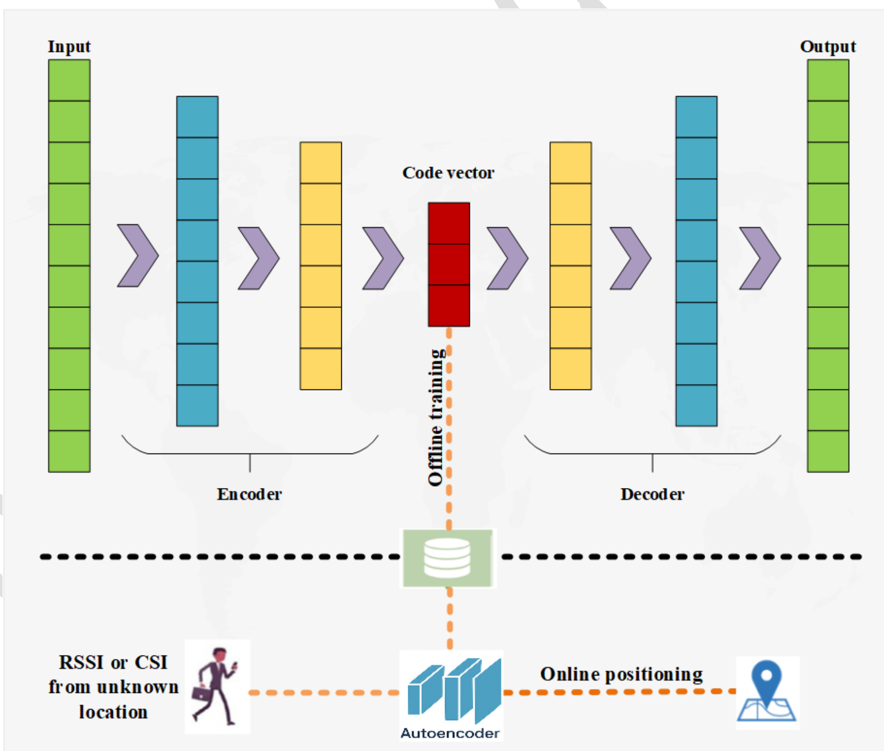

Fig. 1. The proposed system model

implements a nonlinear transformation that projects the input signal into a low-dimensional latent space, while the decoder performs the inverse mapping to reconstruct the input from this latent representation.

In the decoding stage, two layers corresponding to the encoder layers are designed to reconstruct the compressed features. The learning process is driven by the minimization of a reconstruction objective, which enforces that the latent code preserves the most informative structures of the input while suppressing irrelevant variations. Consequently, the autoencoder network can simultaneously extract key features and enable their use in applications such as dimensionality reduction, data analysis, and classification, providing a robust foundation for the proposed indoor localization system.

In the proposed system, this representation learning mechanism is exploited to model the underlying structure of raw Wi-Fi measurements. By constraining the dimensionality and statistical properties of the latent space, the encoder is encouraged to retain only task-relevant features and to attenuate measurement noise and multi-path interference. The decoder, in turn, acts as a consistency constraint, ensuring that the learned latent variables maintain sufficient information to faithfully reconstruct the original signals. As a result, the hidden code captures a compact and discriminative fingerprint that is well suited for fine-grained indoor localization. The precise mathematical definitions of the encoder–decoder mappings, the optimization objective, and the imposed constraints are detailed in Section IV.

3. Non-Smooth Regularization to Prevent Overfitting in Deep Autoencoders

Deep autoencoders require effective regularization mechanisms to prevent overfitting and promote the learning of meaningful latent representations. Overfitting occurs when a learning model captures noise, incidental patterns, or dataset-specific characteristics instead of the underlying data distribution, resulting in excellent performance on training data but poor generalization to unseen samples. In deep autoencoders, this phenomenon is primarily attributed to factors such as high model capacity, excessive network depth, limited or imbalanced training data, and insufficient regularization. As a result, the learned latent representations may become superficial or redundant, reducing the model's ability to capture informative structural features. Consequently, incorporating appropriate regularization is essential for improving generalization performance, enhancing representation quality, and increasing the robustness of deep autoencoder-based localization systems in complex real-world environments.

Overfitting severely limits a model's ability to generalize to unseen data and reduces its practical applicability in real-world scenarios [26]. Although the primary objective of autoencoder training is to reconstruct the input, high-capacity models often tend to memorize the training data rather than capturing the underlying meaningful structure. To address this issue, recent studies have extensively investigated regularization strategies within deep representation learning frameworks, particularly controlled noise injection and sparsity-promoting constraints in the latent space. Noise-based regularization has been shown to enhance robustness and generalization by enforcing smoothness in learned representations, while latent sparsity constraints encourage compact and discriminative feature encoding. These techniques are widely recognized as effective mechanisms for stabilizing the training process of autoencoder-based models and mitigating overfitting in complex and noisy environments, as demonstrated in several studies such as [27-29].

Regularization typically involves augmenting the original loss function with an additional penalty term that enforces structural constraints on the learned parameters. Depending on the chosen norm or functional form of this penalty, the regularization mechanism can promote different properties such as smoothness, energy minimization, or sparsity in the model representation. Mathematically, this leads to an optimization problem defined by a composite objective function that balances data fidelity with constraint enforcement through a tunable regularization coefficient. Such formulations are particularly effective in controlling overfitting and stabilizing learning in high-dimensional settings. The complete mathematical formulation and the specific regularization functions adopted in this study are rigorously derived and discussed in Section IV.

Common approaches include sparse, denoising, contractive, and variational regularization, each promoting more compact, robust, and informative representations [30]. Among them, non-smooth regularizers (e.g., $\ell 1$ based or absolute-value penalties) apply non-differentiable constraints that encourage sparsity and robustness to noise and uncertainty [20, 31]. These regularizers help reduce network redundancy, improve feature interpretability, and enhance resilience to environmental variations, resulting in more stable and discriminative reconstructions.

While traditional smooth regularizers such as $\ell 2$ norm have been extensively studied in deep learning [32-34], the integration of non-smooth regularization such as $\ell 1$, into deep autoencoders for Wi-Fi fingerprint-based indoor localization remains largely unexplored. Given their potential to improve sparsity, interpretability, and generalization, these techniques offer a promising direction for enhancing localization robustness and stability. Nevertheless, incorporating non-smooth terms increases optimization complexity, as these functions are not differentiable and require advanced solvers as well as careful hyperparameter tuning. Large and diverse datasets typically require weaker regularization, while small or noisy datasets benefit from stronger constraints to prevent overfitting. Similarly, excessive regularization in feature-rich environments can suppress informative signals, whereas mild regularization balances flexibility and generalization. These considerations and trade-off between bias and variance are critical for designing deep autoencoder-based localization systems that maintain both accuracy and robustness in real-world indoor environments [35, 36].

Training instability induced by non-smooth regularization remains one of the most important challenges in gradient-based optimization for deep neural networks. Regularization techniques based on non-smooth penalty functions, such as the $\ell 1$-norm, introduce non-differentiable points into the optimization landscape, thereby violating the smoothness assumptions underlying conventional first-order optimization algorithms. As a result, gradient estimates may become inconsistent in the vicinity of non-differentiable regions, leading to oscillatory parameter updates, slower convergence, and increased sensitivity to the selection of hyperparameters, particularly the learning rate. These issues are further exacerbated in deep

10.22060/EEJ.2026.25375.5921

architectures, where optimization is already complicated by highly non-convex loss surfaces and the propagation of gradient information across multiple layers.

To effectively address the optimization challenge posed by the non-smooth regularization term, this study employs the proximal optimization framework, which is specifically designed for composite objective functions containing both smooth and non-smooth components. Instead of directly minimizing the non-differentiable objective, the optimization problem is decomposed into a differentiable gradient update followed by a proximal mapping that provides a closed-form or computationally efficient solution for the non-smooth term. This proximal strategy preserves the sparsity-promoting characteristics of the regularizer while ensuring numerical stability, improving convergence behavior, and mitigating the training instability commonly associated with non-smooth optimization. Consequently, the proposed approach achieves a more robust and reliable training procedure without compromising the effectiveness of the imposed regularization.

4. Mathematical Formulation of the Problem

In practice, an autoencoder is an unsupervised neural network that learns how to efficiently compress input data. It also learns to reconstruct the data from its compressed representation such that the difference between the original and the reconstructed data is minimized.

In the following, to derive the mathematical formulation of the autoencoder training process, let $\mathbf{X}$ denote the input data (i.e., the RSSI or CSI values). The encoder part can be formulated as a function $g(.)$, where its output ($\mathbf{z}_i$) represents the feature space, and it can be expressed as follows:

$$\mathbf{z}_i = g\left(\mathbf{x}_i\right). \tag{1}$$

10.22060/EEJ.2026.25375.5921

The next component of an autoencoder network is the decoder, which represents the output of the autoencoder. It reconstructs the input data from the latent features. The decoder can be formulated as a function $f(.)$ of the hidden representations ($\mathbf{z}_i$), and can be expressed as follows:

$$\hat{\mathbf{x}}_i = f\left(\mathbf{z}_i\right) = f\left(g\left(\mathbf{x}_i\right)\right); \qquad (2)$$

In the training phase of an autoencoder, the objective is to minimize the loss function by obtaining the optimal weight parameters of the network model. This optimization problem can be formulated as follows:

$$\underset{\boldsymbol{\theta}}{arg\,min}\ \mathcal{L}\left(f\left(g\left(\mathbf{x}_i\right), \boldsymbol{\theta}\right), \mathbf{x}_i\right). \qquad (3)$$

In the above expression, $\mathcal{L}(.)$ represents the loss function and measures the reconstruction loss between the input and the output, also, $\boldsymbol{\theta}$ refers to the set of model parameters (i.e., the weights and biases of the autoencoder layers). By training the autoencoder network to minimize the loss function, the optimal parameters can be determined. These optimized parameters are then used during the online phase to predict the indoor location based on newly collected RSSI or CSI values.

Regularization techniques such as $\ell 1$ and $\ell 2$ add a penalty term to the loss function, encouraging the model to maintain smaller parameter values. Specifically, $\ell 1$ regularization promotes sparsity by driving some parameters toward zero, which effectively performs feature selection. In contrast, $\ell 2$ regularization discourages large parameter values, leading to smoother solutions and improved numerical stability.

In other words, applying $\ell 1$-norm regularization in autoencoders enforces sparsity within the network and facilitates the selection of important features. This method adds the absolute magnitude of the network coefficients as a penalty term to the model's loss function. Such a penalty can drive some coefficients to zero, helping the network focus on the most relevant features while ignoring less significant ones.

To apply $\ell 1$-norm regularization to an autoencoder, the following expression must be minimized:

10.22060/EEJ.2026.25375.5921

$$\underset{\boldsymbol{\theta}}{arg\,min}\ \mathbb{E}\left[\Delta\left(\mathbf{x}_i, f\left(g\left(\mathbf{x}_i\right)\right)\right)\right] + \lambda\sum_i |\mathbf{z}_i|, \quad (4)$$

where the operator $\mathbb{E}[.]$ represents the expected value computed over all observations and $\boldsymbol{\theta}$ represents the parameters of the encoder and decoder functions (i.e., the network weights). The scalar term $\lambda > 0$ denotes the regularization coefficient, which determines the magnitude and strength of the $\ell 1$-norm regularization.

Due to the presence of non-smooth and non-differentiable components, an alternative approach known as the proximal method is required to solve the above equation. In the context of autoencoder training, it allows us to efficiently incorporate the non-smooth regularization while still updating the network parameters. By iteratively applying the proximal operator alongside standard gradient-based updates, the model can converge to an optimal solution that balances reconstruction accuracy and sparsity, as well as smoothness of the parameters. We formulate non-smooth regularized autoencoder as:

$$\underset{\boldsymbol{\theta}}{arg\,min}\ \mathbb{E}\left[\Delta\left(\mathbf{x}_i, f\left(g\left(\mathbf{x}_i\right)\right)\right)\right] + \psi(\gamma), \quad (5)$$

where $\psi(\gamma)$ is a non-smooth proximable lower semi-continuous regularizer. γ could be any of network parameters or variables (equivalently $\gamma = f(\mathbf{X};\boldsymbol{\theta})$). To deal with this problem, we introduce new variable α and reformulate (5) as follows:

$$\begin{aligned} &\underset{\boldsymbol{\theta}}{arg\,min}\ \mathbb{E}\left[\Delta\left(\mathbf{x}_i, f\left(g\left(\mathbf{x}_i\right)\right)\right)\right] + \psi(\alpha), \\ &\qquad\qquad subject\ to: \gamma = \alpha \end{aligned} \quad (6)$$

An approximate solution to problem (6) can be obtained through the application of penalty-based optimization techniques [37]. In this framework, the approximation is formulated as follows:

10.22060/EEJ.2026.25375.5921

$$\underset{\boldsymbol{\theta}}{arg\,min}\ \mathbb{E}\left[\Delta\left(\mathbf{x}_i, f\left(g\left(\mathbf{x}_i\right)\right)\right)\right] + \psi(\gamma) + \frac{1}{2\mu}\|\gamma - \alpha\|^2, \qquad (7)$$

where $\mu > 0$ denotes the penalty parameter. As $\mu \to 0$, the solution of the penalized formulation converges to the exact solution of the problem. To ensure convergence, we incorporate the indicator function of the constraint set into the objective function, leading to the following formulation:

$$\underset{\boldsymbol{\theta}}{arg\,min}\ \mathbb{E}\left[\Delta\left(\mathbf{x}_i, f\left(g\left(\mathbf{x}_i\right)\right)\right)\right] + \psi(\gamma) + \frac{1}{2\mu}\|\gamma - \alpha\|^2 + \Phi(\theta), \qquad (8)$$

where the following definitions are employed:

$$\Phi(\theta) \triangleq \begin{cases} 0 & if \quad \|\theta\|_\infty \le M \\ \infty & if \quad \|\theta\|_\infty > M \end{cases} \qquad (9)$$

$\Phi(\theta)$ is also proximal and lower semi-continuous. Following the proximal mapping definition in [38], for a proper, closed, convex function $g : \mathbb{R}^n \to \mathbb{R} \cup \{+\infty\}$ and parameter $\lambda > 0$, the proximal operator is defined as:

$$prox_{\lambda g}(\boldsymbol{\upsilon}) = \underset{\mathbf{x} \in \mathbb{R}^n}{\arg\min}\left(g\left(\mathbf{x}\right) + \frac{1}{2\lambda}\|\mathbf{x} - \boldsymbol{\upsilon}\|_2^2\right). \qquad (10)$$

In particular, for the $\ell 1$ penalty $g\left(\mathbf{x}\right) = \|\mathbf{x}\|_1$, the corresponding proximal mapping is given by the soft-thresholding (shrinkage) operator, which possesses the following closed-form representation [38]:

$$prox_{\lambda\|\cdot\|_1}(\upsilon_i) = sign\left(\upsilon_i\right)\max\left(|\upsilon_i| - \lambda, 0\right), \qquad (11)$$

where v_i means the ith element of $\boldsymbol{v}$. Then, by employing Equations (9)–(11), the proximal mapping of $\beta\left(\Phi(\theta)\right)$ for $\beta > 0$ is calculated by the following term [21]:

10.22060/EEJ.2026.25375.5921

$$prox_{\beta\Phi(\theta)}\left(x_i\right) \triangleq \begin{cases} x_i & if \quad x_i \leq M \\ sign\left(x_i\right).M & if \quad x_i > M \end{cases}. \tag{12}$$

Another approach for applying regularization to an autoencoder network is to add an $\ell 2$-norm regularization term to the loss function. This method adds the squared magnitudes of the coefficients as a penalty term to the loss function. Unlike the $\ell 1$-norm, $\ell 2$ regularization does not force coefficients exactly to zero; instead, it encourages them to take small values.

The optimization problem by considering $\ell 2$ regularization can be expressed as:

$$arg \min_{\boldsymbol{\theta}} \mathbb{E}\left[\Delta\left(\mathbf{x}_i, f\left(g\left(\mathbf{x}_i\right)\right)\right)\right] + \beta \sum_i \boldsymbol{\theta}_i^2. \tag{13}$$

Here again, beta is a positive scalar controlling the strength of the $\ell 2$-norm regularization. In the case of the $\ell 2$-norm, the derivative with respect to the parameters is easily computable, making it straightforward to implement. Note that this advantage applies while the $\ell 1$-norm regularization introduces more challenges in optimization because its penalty function is non-smooth and not differentiable everywhere. Nonetheless, both methods enhance the latent feature representation by introducing sparsity and reducing model complexity.

In summary, $\ell 2$-norm regularization mainly reduces large parameter values in the network's weight matrix, whereas $\ell 1$-norm regularization enforces sparsity by driving many weights to zero and leading to a more compact and interpretable autoencoder structure.

Finally, based on the above explanations, the final formulation for training the autoencoder, considering both the non-smooth and smooth regularization terms, can be expressed as follows:

$$\begin{aligned} & \underset{\boldsymbol{\theta}}{arg\,min}\ \mathbb{E}\left[\Delta\left(\mathbf{x}_i, f\left(g\left(\mathbf{x}_i\right)\right)\right)\right] + \lambda\sum_i |\mathbf{z}_i| + \beta\sum_i \boldsymbol{\theta}_i^2 \\ & = \underset{\boldsymbol{\theta}}{arg\,min}\ \mathbb{E}\left[\Delta\left(\mathbf{x}_i, f\left(g\left(\mathbf{x}_i\right)\right)\right)\right] + \psi(\gamma) + \frac{1}{2\mu}\|\gamma-\alpha\|^2 + \beta\sum_i \boldsymbol{\theta}_i^2 \end{aligned} \tag{14}$$

In the aforementioned formulation, the update rule for variables block $\boldsymbol{\theta}$, By exploiting the principles of proximal optimization and drawing upon the concept of the proximal operator[31], can be formulated in the following form:

$$\theta_{k+1} = prox_{\mu_{\theta,k} r2}\left(\theta_k - \mu_{\theta,k}\nabla_\theta E\left(\theta_k, \alpha_{k+1}\right)\right), \tag{15}$$

where

$$E(\theta,\alpha) = \mathbb{E}\left[\Delta\left(\mathbf{x}_i, f\left(g\left(\mathbf{x}_i\right)\right)\right)\right] + \frac{1}{2\mu}\|\gamma-\alpha\|^2. \tag{16}$$

Then, the update rule for α could be simplified as:

$$\alpha_{k+1} = prox_{\mu\psi}\left(\gamma_k\right). \tag{17}$$

Finally, to solve the formulated non-smooth optimization problem, we will use the Non-Smooth Regularized Autoencoder (NSAE) algorithm. NSAE is a joint optimization framework that alternates between an outer penalty-based iteration and an inner proximal subproblem to train autoencoders with non-smooth regularization. Based on the above formulation, the proposed proximal-based NSAE algorithm is summarized as follows:

Non-Smooth Regularized Autoencoder (NSAE) algorithm

Input	Input data matrix **X**, encoder and decoder mappings g (.), f (.), penalty parameters $\mu_{\max}, \mu_{\min}$, scaling factor α, and termination thresholds ε, ζ.
Initialize	$\theta_0, \alpha_0 = 0$; k = 0; $\mu = \mu_{\max}$
Output	Optimized autoencoder parameters $\theta*$

10.22060/EEJ.2026.25375.5921

Procedure:
Outer Loop (Penalty Update) i=0:
Set Flag ← True
while Flag do
  Inner Subproblem (Proximal Optimization):
    Initialize k = 0
    while Flag and k < Iter_max:
      $\alpha_{k+1} = prox_{\mu}(\gamma_k)$
      $\theta_{k+1} = prox_{\mu}\left(\theta_k - \mu \nabla_{\theta} E(\theta_k, \alpha_{k+1})\right)$
      k ← k + 1
    Check Inner Convergence:
      $||\theta_k - \theta_{k-1}||_2 \leq \epsilon$ then stop inner loop
    Update Outer Variables:
      $\theta_{i+1}, \alpha_{i+1} \leftarrow \theta_i, \alpha_i$
      i ← i + 1
    Penalty Parameter Update:
      $\mu \leftarrow s.\mu$
      $if\ \mu < \mu_{min}\ then\ \mu = \mu_{min}$
    Check Outer Convergence:
      if $||\gamma_i - \alpha_i||_2^2 \leq \zeta$ then Flag ← False

In the *i*-th iteration of the outer loop, the penalty parameter μ is updated as the product of the previous penalty and a scaling factor s (i.e., $\mu \leftarrow s.\mu$), ensuring adaptive control over the strength of sparsity and non-smooth regularization. Within each outer iteration, the inner problem, is solved using proximal gradient mappings that refine the encoder-decoder parameters while handling non-differentiable penalties such as $\ell 1$-norm or structured sparsity terms.

This nested optimization mechanism allows NSAE to balance reconstruction fidelity and regularization constraints, driving the model toward an optimal equilibrium $\boldsymbol{\theta}^*$ where both the data representation and the imposed regularization are jointly satisfied. The proximal operator is adopted because it provides an efficient and numerically stable mechanism for optimizing objective functions containing non-smooth regularization terms. Instead of directly minimizing the non-differentiable objective, the optimization problem is decomposed into a sequence of proximal subproblems, each of which can be solved efficiently while preserving the sparsity-promoting characteristics of the regularization. This strategy improves

10.22060/EEJ.2026.25375.5921

optimization stability and facilitates convergence without compromising the reconstruction capability of the autoencoder.

From an implementation perspective, the optimization process employs an adaptive penalty update strategy, where the penalty parameter is progressively adjusted throughout the outer iterations to achieve a balanced trade-off between reconstruction accuracy and regularization strength. Within each outer iteration, the encoder and decoder parameters are refined through successive proximal updates until the predefined convergence conditions are satisfied. The optimization terminates automatically when both the inner proximal optimization and the outer penalty-update procedure satisfy their respective stopping criteria, ensuring stable convergence while avoiding unnecessary computational overhead.

Overall, this optimization strategy enables the proposed NSAE framework to effectively handle non-smooth regularization in a computationally efficient manner while maintaining stable training behavior, reliable convergence, and high-quality latent feature representations. Furthermore, to facilitate the implementation of the proposed NSAE framework, the penalty parameter (μ) is initialized at 1000 and progressively decreased according to the predefined update schedule [100,10,1,0.1,0.01]. The remaining required parameter values are provided in the Results and Discussion section.

To quantitatively assess the performance of the proposed indoor localization system, the Root Mean Square Error (RMSE) is utilized as the primary evaluation metric. RMSE measures the average magnitude of the localization error by computing the square root of the mean of the squared Euclidean distances between the estimated and ground-truth positions. It can be defined as follows:

$$\mathrm{RMSE} = \sqrt{\frac{1}{N}\sum_{i=1}^{N}\left[(\hat{x}_i - x_i)^2 + (\hat{y}_i - y_i)^2 \right]} = \sqrt{\mathrm{RMSE}_x + \mathrm{RMSE}_y}, \tag{18}$$

where N denotes the total number of test samples, $(\hat{x}_i, \hat{y}_i)$ represents the predicted two-dimensional position of the i-th sample obtained from the network, and (x_i, y_i) corresponds to the associated ground-truth location. The operator $\|\cdot\|_2$ indicates the Euclidean norm.

5. The Results and Discussion

In this section, we evaluate the performance of the proposed localization system based on a deep learning network with a proximal-regularized autoencoder structure. The improvement in localization accuracy is analyzed under different regularization schemes, as well as in the absence of any regularization. The proximal-regularized autoencoder network is implemented on the TensorFlow [39] framework. The parameters and corresponding values used for the implementation of the deep learning-based localization system with the proximal-regularized autoencoder structure are summarized in Table 1. Furthermore, the hardware used for data processing in this study consists of a personal computer equipped with an Intel Core i5 processor, 16 GB of RAM, a 512 GB SSD, and an NVIDIA GTX 1060 graphics card with compute capability 6.1, 6 GB of dedicated memory, and 14 GB of shared memory.

To this end, our proposed method is evaluated using the public RSSI dataset UJIIndoorLoc [40] and CSI dataset that is collected from a controlled indoor environments designed to emulate realistic signal propagation conditions for evaluating localization algorithms [41].

5-1- Results of the proposed localization system using RSSI data

Although numerous research studies have attempted to address the indoor localization problem using WLAN fingerprinting-based methods, a major limitation in this field remains is the lack of a common database for benchmarking and comparison purposes. To overcome this gap, the UJIIndoorLoc dataset

10.22060/EEJ.2026.25375.5921

was introduced [40]. Owing to its high standards, this dataset has become a reference benchmark for evaluating and comparing various WiFi fingerprint-based indoor localization methods.

Table 1. Values and types of parameters used in the simulation

Definition	Values and types
Input size	520
Output size	2
Optimization algorithm	Adam
Activation function of the encoder network	ReLU
Activation function of the last layer of the decoder network	Sigmoid
Loss function	MSE
Percentage of training samples	80%
Percentage of testing samples	20%
Number of encoder layers	2
Number of decoder layers	2
Dimension of the first encoder layer (extracted features)	300
Dimension of the second encoder layer (extracted features)	150

The UJIIndoorLoc database covers three buildings of Jaume I University, each comprising four or five floors, with a total area of approximately 108,703 m^2. The dataset was collected by more than 20 different users using 25 Android devices. It contains 19,937 training records and 1,111 validation records. A total of 529 features are recorded for each fingerprint such as Wi-Fi fingerprints, the coordinates of the fingerprint's recording location, and other useful metadata. Each Wi-Fi fingerprint is described by the identified Wireless Access Points (WAPs) and their corresponding RSSI values. RSSI values are recorded as integer dBm values ranging from -104 dBm (very weak signal) to 0 dBm. A positive value of 100 is used to indicate that a given WAP was not detected.

During dataset creation, 520 distinct WAPs were identified. Consequently, out of the 529 fingerprint features, 520 are RSSI measurements. The geographic coordinates (longitude and latitude) of the measurement location are then stored. Additional features include the building and floor identifiers and

10.22060/EEJ.2026.25375.5921

metadata about who recorded the Wi-Fi (user), how it was recorded (Android device and OS version), and when it was recorded (timestamp).

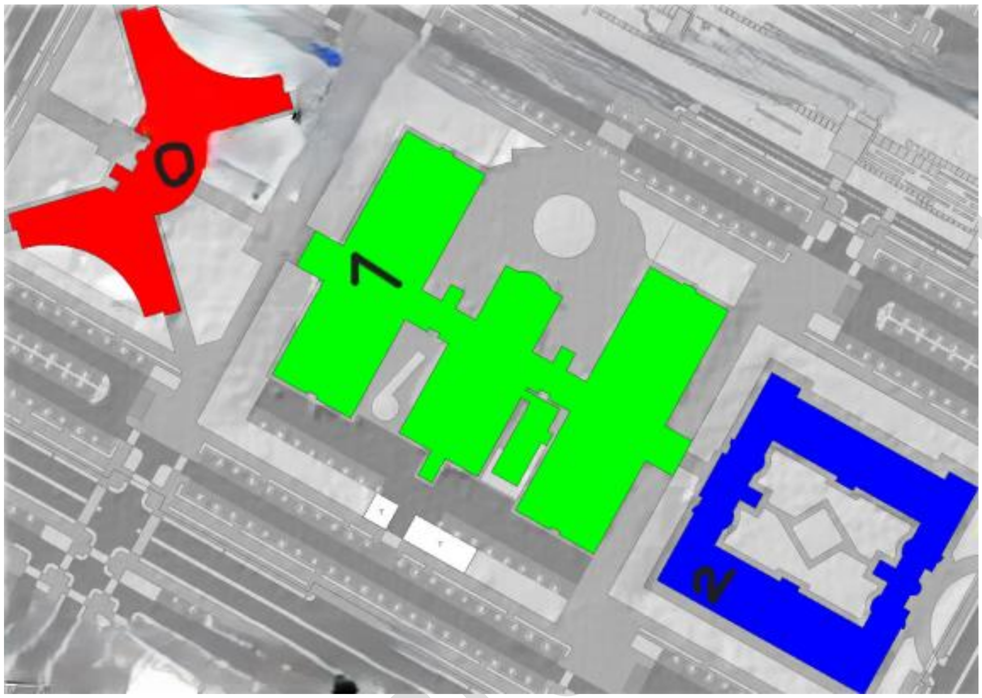

Fig. 2. Map of the three buildings at Jaume I University on which the UJIIndoorLoc database is based, covering an area of approximately 108,703 m^2 [40].

To address the regression problem of estimating true geographic longitude and latitude using the dataset shown in Fig. 2, we first isolate the reference points located in Building 1, Floor 1 as illustrated in Fig. 3. Next, the proximal-regularized autoencoder network is trained according to the methodology described in Sections 3 and 4. In the online localization phase, RSSI measurements are collected at an unknown location and fed into the trained autoencoder to obtain a low-dimensional representation. This representation is compared with the nearest match in the fingerprint database, and the location associated with the best match is returned as the estimated position.

For UJIIndoorLoc dataset, the designed autoencoder network in this study has an input dimension of 520, aiming to capture and reconstruct latent patterns in the RSSI data. It consists of two encoder layers and

10.22060/EEJ.2026.25375.5921

two corresponding decoder layers. During encoding, the input is first reduced from 520 to 300 features and then further compressed to 150 features in the second layer.

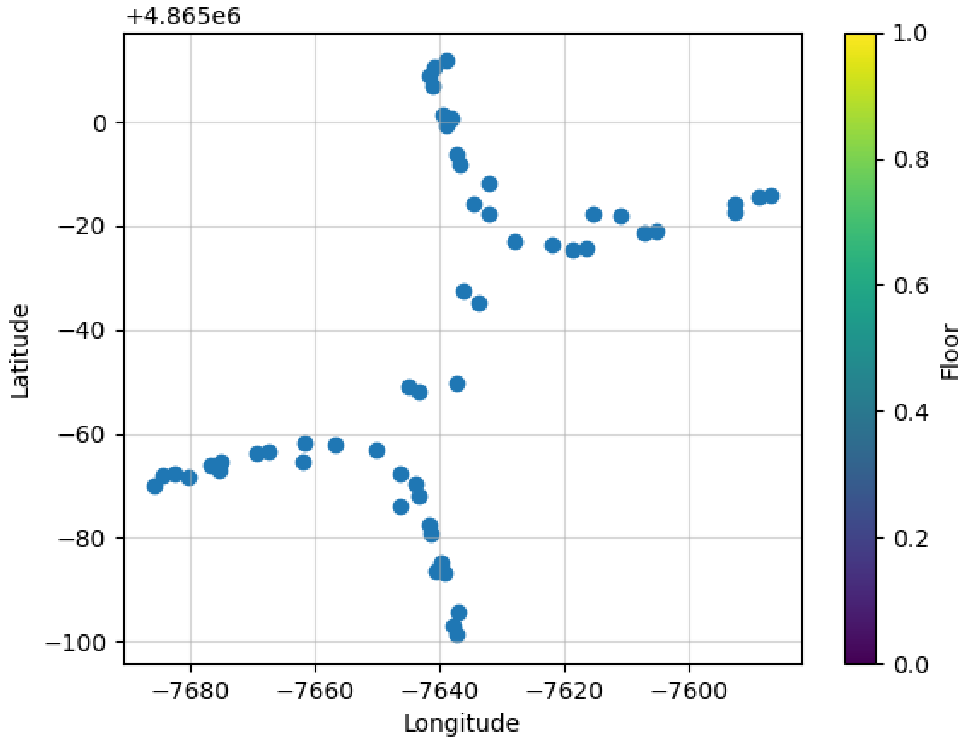

Fig. 3. The process of separating reference points in the UJIIndoorLoc database (Building 0 in Fig. 2, first floor) for solving the regression problem and estimating the actual latitude and longitude coordinates.

This gradual compression allows the network to learn an optimized low-dimensional representation. The network is trained using the Adam optimization algorithm, with ReLU activation functions in the hidden layers to accelerate convergence and enhance nonlinear feature extraction.

The final decoder layer employs a Sigmoid activation to ensure reconstructed outputs fall within a normalized and interpretable range. For performance evaluation, the RSSI or CSI dataset is split into

10.22060/EEJ.2026.25375.5921

training and testing subsets, with 80% of the samples used for training and 20% reserved for testing. This split ensures that the model not only learns effectively but also demonstrates generalization capability.

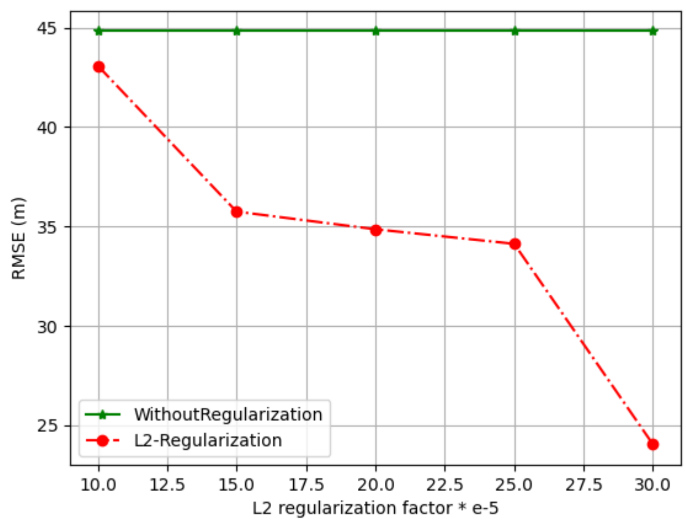

Fig. 4. Comparison of the RMSE of the deep autoencoder–based indoor localization system without regularization and with regularization during online position estimation as a function of the $\ell 2$ regularization magnitude (β).

Fig. 4 presents the performance of the deep autoencoder–based positioning system under two configurations: without regularization and with $\ell 2$ regularization applied during coordinate estimation. The curve associated with $\ell 2$ control shows a monotonic error-decay behavior as the regularization magnitude β increases, particularly in higher regimes, indicating improved stability of latent position codes and enhanced noise-robust coordinate regression. In contrast, the unregularized model saturates at a high RMSE level (≈45 m) and remains nearly insensitive to β, demonstrating the lack of effective constraints on iterative position updates. The pronounced RMSE reduction at larger β values suggests better conditioning of the decoder's inverse spatial mapping from latent embeddings to physical coordinates, mitigating coordinate drift and reducing cumulative spatial deviation. These results confirm

10.22060/EEJ.2026.25375.5921

that $\ell 2$ regulation function improve metric-level localization fidelity by minimizing the gap between predicted and ground-truth positions. Fig. 5 further illustrates the localization error of the proposed deep autoencoder–based system with and without the incorporation of non-smooth regularization, again

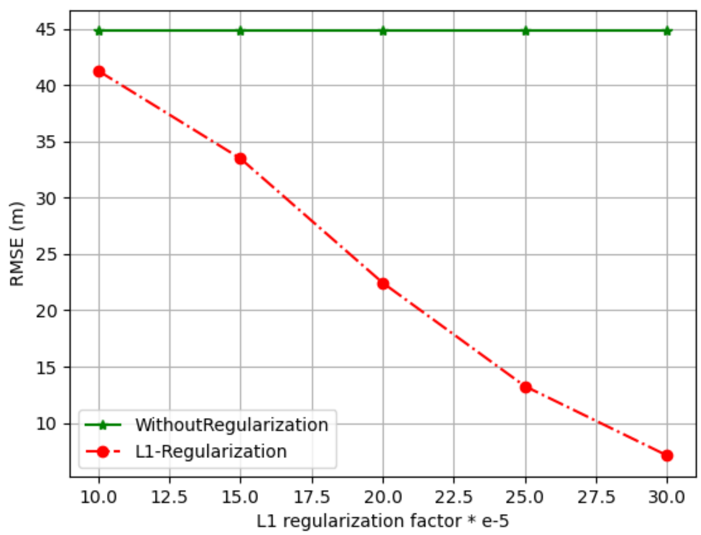

Fig. 5. Comparison of the RMSE of the deep autoencoder–based localization system without regularization and with regularization during online position estimation as a function of the $\ell 1$ regularization magnitude (λ).

evaluated in terms of RMSE as a function of λ. As evident from the results, increasing the regularization strength leads to a consistent decline in localization error. Specifically, in the absence of the non-smooth regularizer, the system exhibits an average localization error of approximately 44.823 m, however, by

applying the non-smooth regularization technique, this error is significantly reduced to nearly 6.78 m, indicating a remarkable improvement in the robustness and precision of the localization framework.

Figures 6 and 7 respectively illustrate the impact of incorporating smooth and non-smooth regularization terms on the performance of the deep autoencoder–based localization system across different numbers of

10.22060/EEJ.2026.25375.5921

training epochs. As is clearly observed, regardless of whether the regularization term (λ or β) is applied to the network, increasing the number of epochs consistently leads to a reduction in RMSE. For instance, when the number of epochs reaches 20, the RMSE in the case without regularization is approximately 30.802 m, while applying the smooth regularization reduces it to 24.169 m, and employing the non-smooth regularization further decreases it to 21.634 m. Similarly, when the number of epochs increases to 30, the RMSE values decline to 28.624 m without regularization, 17.076 m with smooth regularization,

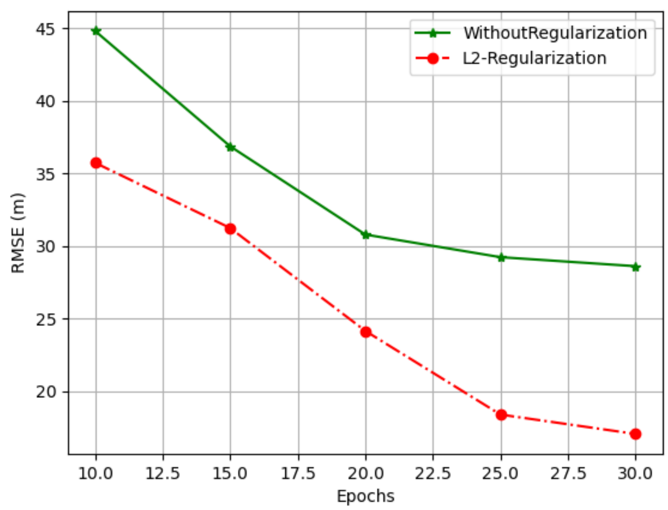

Fig. 6. Comparison of the RMSE of the deep autoencoder–based localization system without regularization and with $\ell 2$ regularization during online position estimation as a function of the number of training epochs.

AUT Journal of Electrical Engineering
10.22060/EEJ.2026.25375.5921

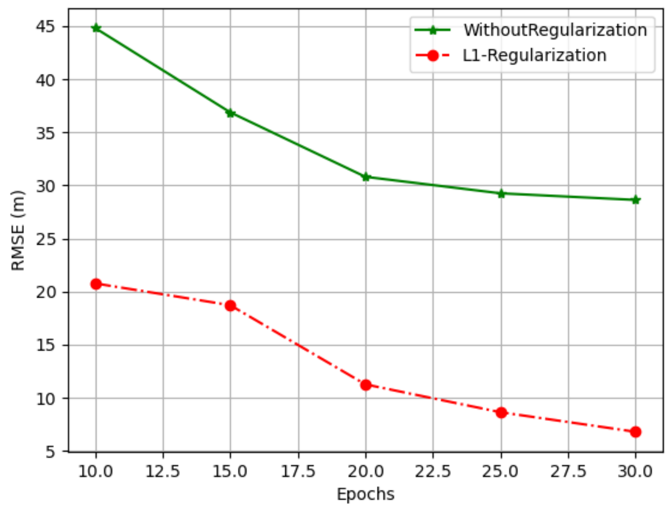

Fig. 7. Comparison of the RMSE of the deep autoencoder–based localization system without regularization and with $\ell 1$ regularization during online position estimation as a function of the number of epochs.

and 8.563 m with non-smooth regularization. These results confirm that both forms of regularization contribute to enhanced learning stability and improved localization accuracy, with the non-smooth regularization demonstrating a notably superior effect in minimizing estimation error.

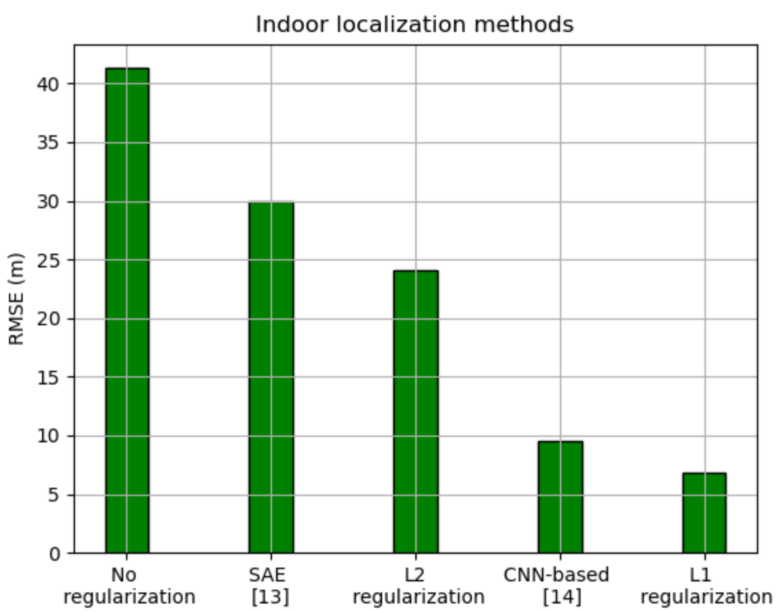

10.22060/EEJ.2026.25375.5921

Fig. 8. Comparison of the RMSE of the deep autoencoder–based localization system with smooth and non-smooth regularization (λ = 30) against other methods reported in the introduction section, evaluated on the UJIIndoorLoc database.

Fig. 8 presents a comparative analysis of the performance of several indoor localization methods. As shown, the localization approach based on a deep autoencoder without regularization (Non-Regularization) exhibits the highest positioning error of 44.82 m, indicating relatively low accuracy. The method reported in [13], which employs a SAE for dimensionality reduction along with a weighted loss function, achieved a localization error of 29.9 m on the UJIIndoorLoc dataset.

By introducing a smooth regularizer, the localization error is significantly reduced to 24.03 m. More recent approaches, such as the method in [14] (which utilizes an advanced convolutional neural network architecture) have demonstrated improved performance on the UJIIndoorLoc dataset, achieving an error of 9.5 m. Finally, as illustrated in the figure, the proposed deep learning–based localization system with a non-smooth regularized autoencoder achieves the lowest localization error of 6.78 m, clearly outperforming existing methods in terms of accuracy and robustness in indoor positioning.

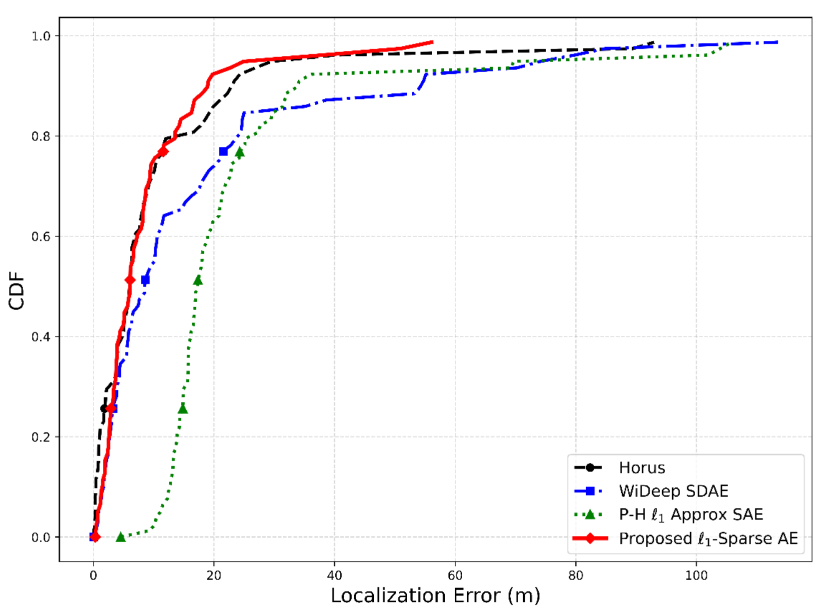

10.22060/EEJ.2026.25375.5921

Fig. 9. Comparison of CDFs of different algorithms for indoor localization.

Fig. 9 illustrates the cumulative distribution function (CDF) of the localization error for four localization approaches, namely the probabilistic Horus method [42], the deep learning-based WiDeep architecture employing a stacked denoising autoencoder (SDAE) [43], the Pseudo-Huber approximation-based sparse autoencoder, and the proposed method. The CDF provides a comprehensive statistical comparison of localization performance over the entire test dataset, allowing the robustness, accuracy, and generalization capability of each method to be evaluated. As shown in the figure, the proposed approach consistently exhibits the leftmost CDF curve, indicating that a larger proportion of test samples are localized with lower positioning errors than the competing methods.

The favorable performance of the proposed approach can be attributed to the integration of $\ell 1$-norm-based sparsity regularization, proximal optimization, and the proposed learning strategy. By preserving dominant and stable RSSI features while suppressing noisy and less informative components, the proposed framework learns a more discriminative latent representation, which contributes to improved spatial separation among fingerprints and reduced overlap between neighboring reference points. As a result, the proposed method achieves lower localization error and demonstrates robust performance under the evaluated experimental conditions. Among the compared methods, Pseudo-Huber exhibits the largest localization error, which may be attributed to the sensitivity of its probabilistic framework to RSSI fluctuations, multipath propagation, and temporal environmental variations, limiting its ability to capture complex nonlinear relationships.

WiDeep SDAE improves localization accuracy by learning nonlinear RSSI representations; however, the absence of an explicit sparsity constraint may allow less informative latent features to remain in the learned representation. Similarly, the Horus method provides competitive localization performance but achieves higher localization error than the proposed approach in the conducted experiments. Overall, the experimental results indicate that the proposed combination of $\ell 1$-based sparse representation and

10.22060/EEJ.2026.25375.5921

proximal optimization provides favorable localization performance for the considered indoor localization scenarios while maintaining robustness against measurement noise and environmental variations.

Table 2 summarizes the statistical characteristics of the localization errors obtained by the evaluated methods. The reported metrics include the mean localization error, which reflects the overall positioning accuracy across all 78 test reference points, the median error, which provides a robust measure of the central tendency by reducing the influence of extreme observations, and the 90th percentile, which represents the error threshold below which 90% of the localization estimates are contained.

These complementary statistics provide a comprehensive assessment of both the average performance and the consistency of each localization algorithm. The experimental results reveal that the Horus probabilistic localizer achieves the lowest mean localization error among all evaluated approaches. This outcome is expected because Horus explicitly models the probabilistic distribution of RSSI measurements at each reference location and performs localization through maximum a posteriori (MAP) estimation. In contrast, deep learning-based autoencoders must simultaneously learn both the latent representation of RSSI fingerprints and the nonlinear mapping to physical locations from finite and noisy training data, making them more susceptible to overfitting or underfitting. Future research may benefit from employing

Table 2. Statistical analysis of localization accuracy across different methods

Method	Mean (m)	Median (m)	90_{th} percentile (m)	RMSE (m)
Horus	10.53	6.65	21.29	15.3
WiDeep SDAE	22.02	15.68	49.79	27.85
P-H $\ell 1$ Approx. SAE	28.77	24.78	56.48	35.10
Proposed NSAE	6.78	5.54	18.33	8.563

10.22060/EEJ.2026.25375.5921

variational autoencoders (VAEs), which explicitly model the underlying probability distribution of the input data and therefore have the potential to improve localization accuracy under uncertain wireless environments. Furthermore, although Horus provides superior average accuracy, its computational complexity during the online localization stage is substantially higher. Specifically, the average inference time is approximately 0.018 s per sample, whereas all deep learning models require only about 0.042 ms, highlighting the considerable computational efficiency and practical suitability of deep neural network-based localization systems for real-time deployment.

A detailed comparison of the deep learning approaches further demonstrates the effectiveness of the proposed $\ell 1$-sparse Autoencoder. The proposed method reduces the mean localization error by 49.46% compared with WiDeep SDAE and by 61.29% relative to the Pseudo-Huber $\ell 1$ Approximation SAE, confirming the benefit of incorporating exact sparsity through proximal optimization rather than relying on smooth approximations of the $\ell 1$ norm. Interestingly, the conventional WiDeep SDAE also achieves lower localization error than the Pseudo-Huber-based sparse autoencoder in the evaluated experiments, suggesting that approximating the $\ell 1$-regularization term does not necessarily improve the discriminative capability of the learned latent representation. These observations indicate that preserving the sparsity-inducing property of the $\ell 1$ norm can contribute to learning more informative latent features under the considered experimental conditions. Furthermore, Table 2 shows that although Horus attains a lower mean localization error, it exhibits a higher RMSE than the proposed method. This observation may

Table 3. Quantitative results for the repeated trials (Mean ± Std) (m)

Method:	**Horus**	**WiDeep SDAE**	**P-H $\ell 1$ Approx. SAE**	**Proposed NSAE**
Value:	10.53± 1.7	22.02± 2.39	28.77± 1.95	6.78 ± 1.38

indicate that Horus produces larger error variations across the evaluated test samples, whereas the proposed $\ell 1$-sparse Autoencoder yields more stable localization performance while maintaining

10.22060/EEJ.2026.25375.5921

competitive average localization accuracy. The reported results are limited to the evaluated datasets and experimental settings.

The repeatability of the evaluated methods was investigated through multiple independent trials to assess the consistency of the obtained localization results. Table 3 summarizes the statistical performance of the compared approaches by reporting the mean localization error along with the corresponding standard deviation obtained from repeated experiments.

These statistical indicators provide additional information about the variability of the results and reflect the degree of stability of each method under repeated evaluations. Such an analysis complements the conventional performance assessment and offers a more reliable interpretation of the experimental outcomes. By considering both the average performance and the associated variation, the robustness and consistency of the compared approaches can be better evaluated.

5-1-1 Computational complexity analysis of deep autoencoders with non-smooth regularization in the proposed localization system

The computational efficiency of an indoor localization framework is a key factor in determining its practicality and scalability for real-world deployment. In addition to localization accuracy, both computational and memory requirements must be carefully considered to assess the feasibility of implementing deep learning models in resource-constrained environments. Accordingly, this section, provides a more comprehensive discussion of the computational complexity and practical implementation

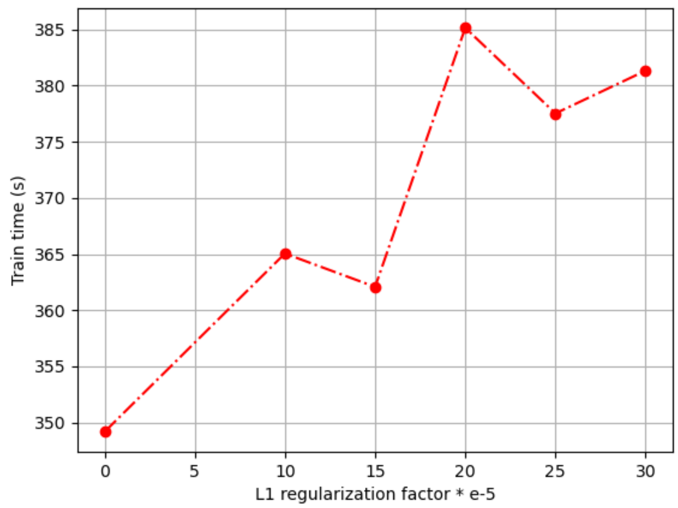

Fig. 10. Analysis of the time complexity of the proposed deep autoencoder–based localization system with regularization, as a function of the regularization magnitude (training time of the deep autoencoder model).

cost of the proposed non-smooth regularized autoencoder, addressing both the offline training phase and the online localization phase.

The proposed framework consists of two computationally distinct stages. The offline stage involves training the deep autoencoder using the Adam optimizer together with the proposed non-smooth regularization strategy. The computational complexity of this phase is primarily determined by the number of training samples, the dimensionality of the input fingerprints, the network depth, the number of neurons in each hidden layer, and the total number of optimization iterations. Although the incorporation of the non-smooth regularization introduces an additional optimization constraint, the resulting computational overhead is confined to the offline training stage, which is executed only once during model construction. In contrast, the online localization stage requires only a forward propagation through the trained network, resulting in a low computational burden that is well suited for real-time indoor positioning applications.

10.22060/EEJ.2026.25375.5921

The computational behavior of the proposed framework is further analyzed through the results presented in Fig. 10, which illustrates the relationship between the regularization coefficient (λ) and the training time. As the regularization strength increases, the optimization problem becomes progressively more constrained,

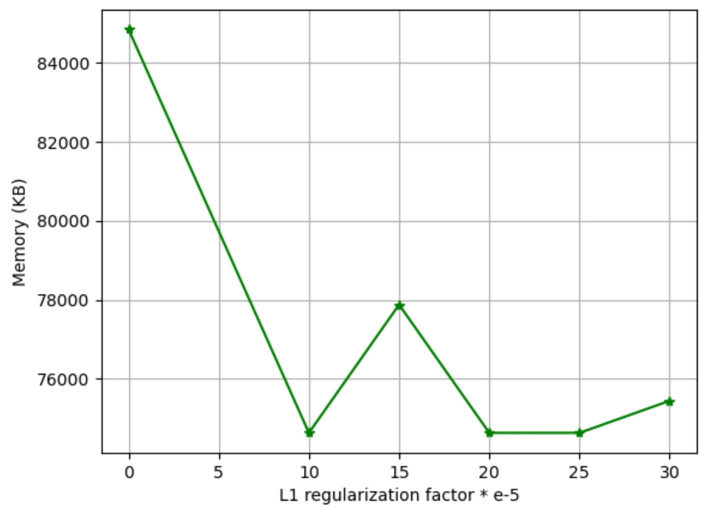

Fig. 11. Analysis of the spatial complexity of the proposed deep autoencoder–based localization system with regularization, as a function of the regularization magnitude (memory consumption).

leading to a nonlinear increase in training time. For relatively small values of λ, the additional computational cost remains negligible. However, larger regularization coefficients increase the complexity of the optimization landscape and require additional iterations to achieve convergence. This behavior reflects the trade-off between computational effort and the enhanced sparsity, robustness, and localization accuracy provided by the proposed regularization strategy.

In addition to temporal complexity, the spatial complexity of the proposed framework has also been analyzed. Memory consumption is primarily associated with storing network parameters, intermediate feature representations, gradients, and activation maps during both training and inference. As illustrated in Fig. 11, the application of non-smooth $\ell 1$ regularization promotes sparse latent representations by driving a substantial number of latent coefficients toward zero. This sparsity reduces the effective storage requirements

10.22060/EEJ.2026.25375.5921

and improves the efficiency of matrix operations, thereby lowering the overall memory footprint while simultaneously enhancing feature discriminability and model generalization. These characteristics improve the scalability of the proposed framework, particularly for large-scale indoor localization scenarios involving high-dimensional fingerprint data.

Overall, the proposed NSAE method achieves a favorable balance between localization accuracy and computational efficiency. Although the regularization mechanism introduces a moderate increase in the computational cost during the offline optimization process, it does not impose a significant overhead during online operation, where only a single forward pass through the trained network is required. Consequently, the proposed method preserves real-time inference capability while offering improved robustness, enhanced generalization, and superior localization accuracy. The expanded discussion of the computational complexity and practical implementation cost therefore demonstrates that the proposed framework is not only accurate but also computationally efficient and suitable for practical indoor localization applications.

5-1-2 Robustness Analysis of the Proposed Localization System Against Noise and Error Sources

The performance of $\ell 1$-regularized autoencoder-based indoor localization systems is inherently influenced by the dynamic characteristics of wireless propagation environments and the quality of the collected fingerprint measurements. In practical deployments, RSSI fingerprints are subject to numerous sources of uncertainty, including multipath propagation, shadowing, temporal signal fluctuations, Radio-Frequency (RF) interference, and hardware heterogeneity among user devices. Moreover, environmental dynamics such as furniture relocation, changes in room layout, door opening and closing, and varying human occupancy continuously modify the radio propagation characteristics, resulting in distribution shifts between the training and testing fingerprints. These factors reduce the consistency of the learned latent representations and may consequently degrade localization accuracy. From a representation learning perspective, maintaining a latent space that is simultaneously discriminative and robust against these perturbations remains one of the principal challenges in fingerprint-based indoor localization.

10.22060/EEJ.2026.25375.5921

The incorporation of $\ell 1$ regularization provides an effective mechanism for improving robustness by enforcing sparse latent representations and suppressing redundant or noisy features. Since only a limited subset of access points typically carries reliable location-discriminative information, sparse regularization encourages the network to preserve these dominant signal components while eliminating weak, unstable,

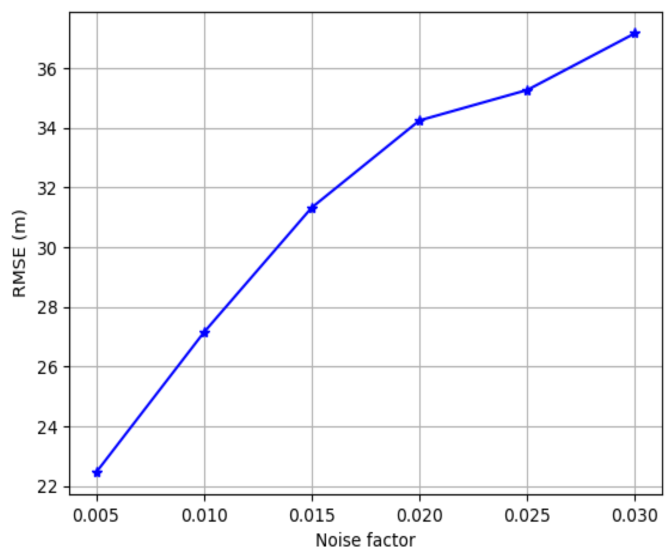

Fig. 12. Evaluation of the effect of increasing noise on the performance of the proposed deep autoencoder-based Indoor localization system with $\ell 1$ regularization as a function of noise magnitude.

and highly correlated RSSI measurements. As a result, the learned feature space exhibits improved separability between neighboring reference points, enhanced resistance to device-dependent signal variations and reduced sensitivity to random measurement noise. In addition, sparse feature learning alleviates overfitting by preventing the latent representation from encoding insignificant environmental artifacts, thereby improving the generalization capability of the localization model across different devices and operating conditions. Consequently, $\ell 1$ regularization contributes not only to higher localization accuracy but also to greater stability under moderate environmental and hardware variations.

10.22060/EEJ.2026.25375.5921

Nevertheless, the effectiveness of sparse regularization is not unlimited. Under highly dynamic indoor environments characterized by severe RF interference, extensive structural modifications, dense human mobility, or substantial changes in the wireless infrastructure, the statistical properties of RSSI fingerprints may deviate significantly from those observed during training. In such cases, even sparse latent representations cannot fully compensate for the resulting distribution mismatch, and localization performance inevitably deteriorates.

This phenomenon is illustrated in Fig. 13, where the localization error (RMSE) increases monotonically as the injected noise level becomes larger. The observed trend demonstrates that although the proposed $\ell 1$-regularized autoencoder exhibits considerable resilience against moderate signal perturbations, excessive noise progressively degrades the quality of the extracted latent features and weakens their discriminative capability. These findings emphasize that combining non-smooth sparse regularization with complementary robustness-enhancement techniques—such as adaptive fingerprint updating, domain adaptation, self-supervised representation learning, or data augmentation—constitutes a promising direction for developing highly reliable indoor localization systems capable of operating in realistic and continuously evolving wireless environments.

5-2- Results of the proposed localization system using CSI data

The experimental evaluations were conducted in a computer laboratory with approximate dimensions of 13.5×11 m², as illustrated in Fig. 13. The environment includes several tables, chairs, and physical obstacles, representing a NLOS propagation scenario. For each sampling position, the CSI of Wi-Fi signals was recorded, containing both real and imaginary parts of the complex channel coefficients. In total, 317 sampling locations were uniformly distributed across the laboratory area, each providing a CSI tensor of size $3 \times 30 \times 1500$, corresponding to three receiving antennas, thirty OFDM subcarriers, and 1500 packets. These measurements formed the foundational dataset for training and evaluating the proposed indoor localization model.

In this part, a deep-learning-based localization framework by leveraging a NSAE will be used to effectively learn spatial representations from high-dimensional CSI data. The NSAE integrates a sparsity-inducing proximal operator into the latent space of the autoencoder, enabling the network to disentangle and preserve essential propagation features while suppressing noise and irrelevant variations. During training, the model jointly minimizes a reconstruction loss and a proximal regularization term, which enforces structured sparsity and enhances feature interpretability.

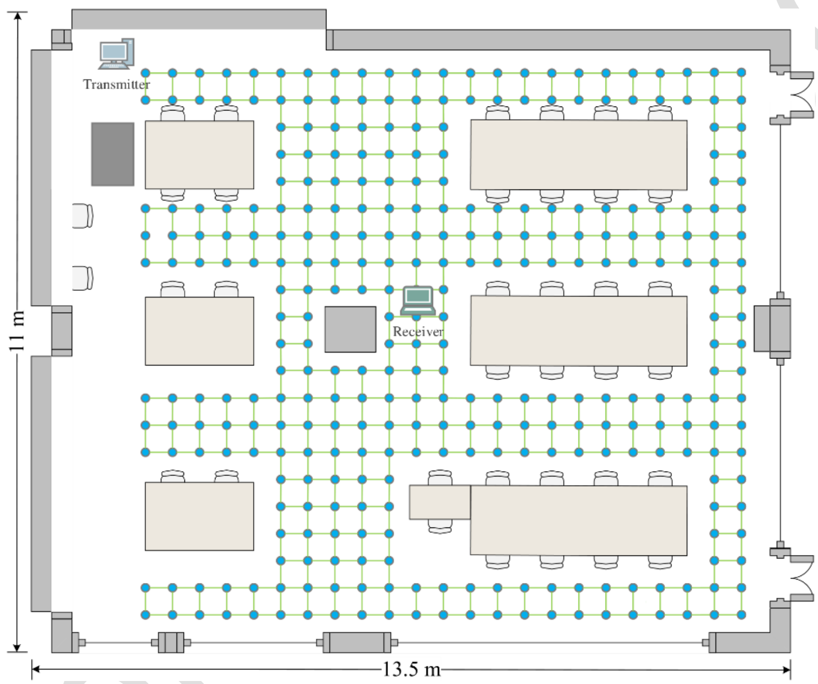

Fig. 13. Floor plan of the computer laboratory used for CSI-based indoor localization under NLOS conditions with 317 sampling points and area of 13.5 × 11 m² [41].

The learned latent representations are subsequently used to estimate the spatial coordinates of each sampling point. This proximal learning strategy allows the model to robustly capture nonlinear relationships between the complex-valued CSI features and their corresponding physical locations, making it particularly effective in NLOS indoor environments characterized by multipath and interference.

The performance of the proposed localization system was evaluated using the RMSE criterion. Experimental results demonstrated that the NSAE achieved an average localization error of approximately 1.73 m within the cluttered laboratory environment. The generated localization error heatmap overlaid on the floor plan revealed that the highest positioning errors occurred in regions with dense obstacles and severe multipath effects. The NSAE-based model successfully extracts spatially discriminative features from CSI data, enabling reliable localization in NLOS indoor environments affected by severe multipath and NLOS signal propagation. The system achieves a final localization error of 1.73 m, demonstrating its capability to maintain accurate position estimation in challenging indoor NLOS conditions.

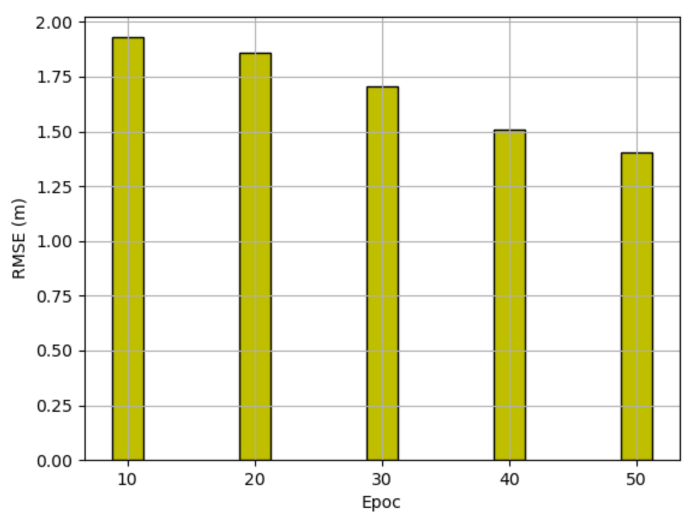

Fig. 14. RMSE trend of the CSI-based indoor localization model across training epochs in a NLOS indoor environment, showing gradual performance improvement with more training.

In addition to these results, the analysis of the NSAE's training dynamics indicates that the model progressively refines its understanding of the underlying CSI–location relationships as learning advances. Early training stages mainly capture coarse spatial patterns, while later epochs enable the network to isolate fine-grained propagation characteristics that are critical for distinguishing closely spaced sampling points. This gradual improvement highlights the ability of proximal regularization to guide the model toward more stable and noise-resistant representations, ultimately enhancing localization accuracy in highly cluttered indoor environments.

Fig. 14 illustrates the performance of a CSI-based indoor localization system deployed in a 13.5 × 11 m² NLOS laboratory environment containing desks, chairs, and other obstructions. The dataset includes 317 sampling points distributed across the area, making the localization task challenging due to severe multipath effects and signal distortion. As the number of training epochs increases, the model learns a more robust mapping between CSI features and spatial coordinates, gradually reducing positioning error. According to the plotted results, the lowest localization error occurs at epoch 50, achieving an RMSE of approximately 1.73 m. This improvement highlights the benefit of longer training for capturing the

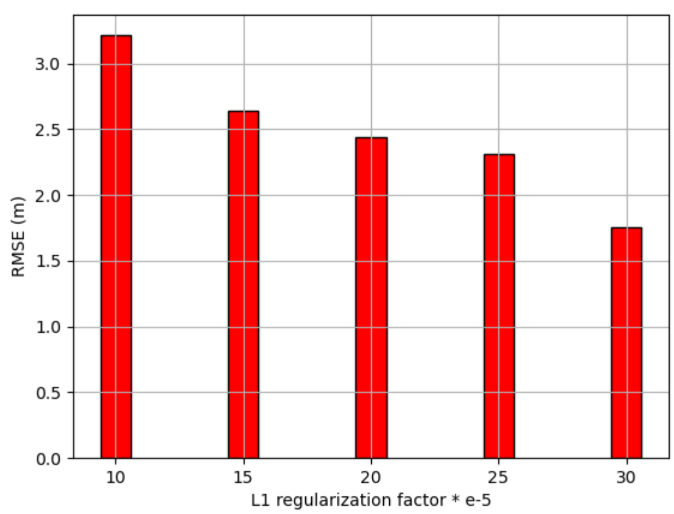

Fig. 15. Variation of the indoor localization RMSE with respect to the $\ell 1$ regularization coefficient (λ) in the CSI-driven indoor localization model, illustrating the influence of the sparsity constraints under NLOS propagation conditions.

complex propagation characteristics typical in NLOS indoor environments. Although the error decreases consistently with more epochs, the curve suggests that further optimization or regularization might still enhance accuracy in highly cluttered spaces. Early epochs struggle to form a stable representation of the wireless channel due to noise, fading, and the irregular geometry of the room. As training progresses, the autoencoder becomes increasingly capable of extracting meaningful latent features that correlate with physical positions. This gradual refinement explains the continuous decrease in RMSE and demonstrates that the model is effectively adapting to the complex NLOS propagation patterns present in the 317-point dataset.

The RMSE profile illustrated in Fig. 15 demonstrates a clear downward trend as the $\ell 1$ regularization magnitude (λ) increases, highlighting the regulatory role of sparsity-inducing penalties in CSI-based indoor localization. In a complex NLOS environment (where multipath propagation, scattering, and noise significantly distort the channel responses) the incorporation of $\ell 1$ regularization effectively suppresses redundant or unstable features within the high-dimensional CSI representation. This progressive reduction in RMSE indicates that stronger sparsity constraints guide the model toward extracting only the most discriminative propagation characteristics, thereby improving its generalization capability and robustness against environmental variability.

Moreover, the monotonic decrease in the localization error, from approximately 3.2 m to around 1.73 m across the examined range of λ, confirms that an appropriately scaled regularization term plays a decisive role in stabilizing the latent representations learned by the network. By imposing structured sparsity constraints the model mitigates overfitting and enhances its ability to disentangle meaningful spatial cues

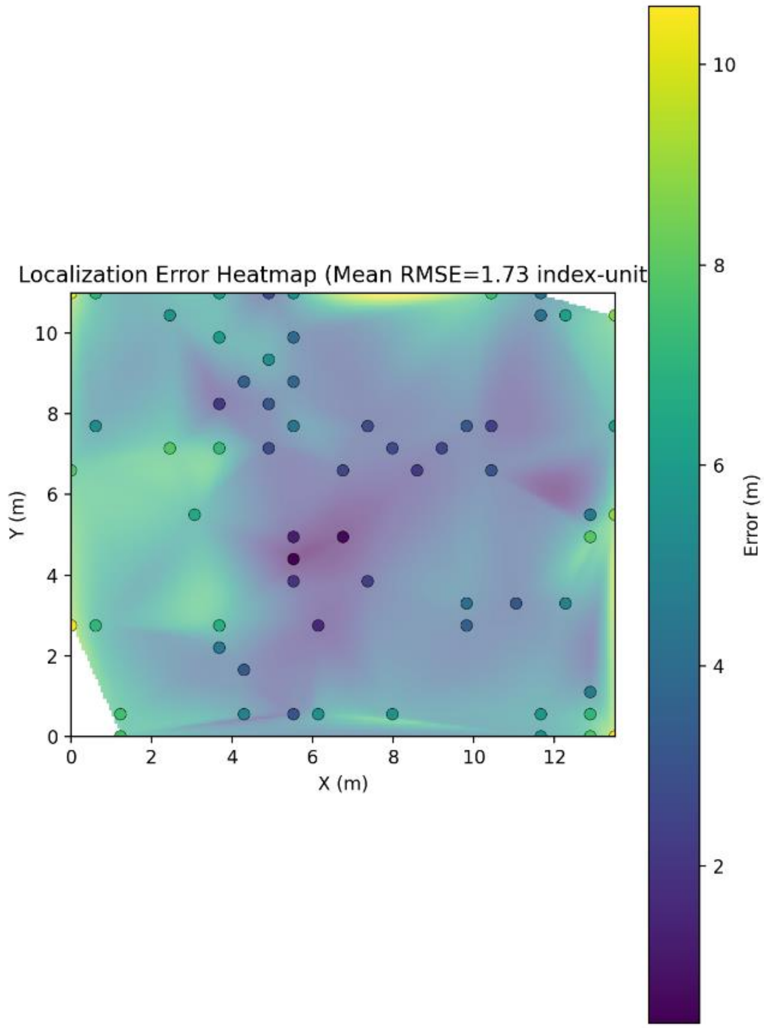

Fig. 16. Localization error heatmap generated by the NSAE model trained on CSI data. The color intensity represents the magnitude of positioning error across the 13.5 × 11 m² laboratory area, with darker regions indicating higher accuracy and lighter areas corresponding to increased localization error due to multipath and NLOS effects.

from noisy measurement artifacts inherent to NLOS conditions, validating that tuning the regularization strength is a critical factor for achieving high-precision and reliable deep learning-based indoor localization using CSI data.

Fig. 16 presents the localization error heatmap obtained from the deep learning–based NSAE model trained on CSI data. The horizontal and vertical axes represent the physical dimensions of the experimental laboratory in meters, while the color scale indicates the magnitude of localization error.

10.22060/EEJ.2026.25375.5921

Darker regions correspond to areas with higher positioning accuracy, whereas lighter tones denote regions of increased estimation error.

As observed, localization accuracy degrades in areas containing dense obstacles or severe multipath reflections, which distort the received CSI patterns. In contrast, open regions with stronger LOS propagation exhibit lower errors. The overall root mean square error (RMSE ≈ 1.73 m) reflects the model's capability to learn spatial signal patterns from high-dimensional CSI data, while highlighting the inherent challenges of achieving sub-meter precision in complex NLOS indoor environments.

6. The conclusion

In this study, a deep learning–based indoor localization system was developed using an autoencoder architecture enhanced with the non-smooth regularization to derive compact and discriminative representations of RSSI or CSI data. The proposed framework operates in two phases: during offline training, the autoencoder learns an efficient low-dimensional mapping of RSSI or CSI fingerprints collected from multiple access points, while in the online phase, newly observed RSSI or CSI values from unknown locations are projected into the learned feature space to estimate user positions. Experimental evaluations demonstrated that incorporating non-smooth regularizers within the autoencoder structure substantially reduces localization error, leading to a more accurate and stable positioning performance compared to traditional and smooth-regularized models.

Future works can extend this research by exploring hybrid localization strategies that integrate multi-source information, such as CSI and sensor data, or by employing ensemble architectures combining multiple deep learning paradigms. Additionally, designing lightweight and energy-efficient deep models suitable for deployment on mobile and embedded platforms would enhance the practicality of the system. The proposed approach shows strong potential for real-world applications such as indoor navigation, IoT-based tracking, and energy management. Nonetheless, further efforts are required to address limitations such as sensitivity to environmental dynamics and the dependency on large-scale labeled datasets.

References

[1] R. Gao, X. Li, and W. Chen, "A Semi-Supervised Indoor Localization Algorithm Based on Probabilistic Distribution Modeling," *IEEE Transactions on Mobile Computing*, 2025, doi: 10.1109/TMC.2025.3608276.

[2] W. Long *et al.*, "Reliable Indoor Localization in Multibuilding Environments: Leveraging Environment-Invariant and Position-Related Features," *IEEE Internet of Things Journal*, vol. 12, no. 14, pp. 26401-26414, 2025, doi: 10.1109/JIOT.2025.3561500.

[3] P. Park, P. D. Marco, and F. Santucci, "Efficient Data Collection and Training for Deep-Learning-Based Indoor Vehicle Navigation," *IEEE Internet of Things Journal*, vol. 11, no. 11, pp. 20473-20485, 2024, doi: 10.1109/JIOT.2024.3371385.

[4] Z. Wei, Z. Zhou, S. Yu, and J. Chen, "Enhanced Indoor Positioning Using RSSI and Time-Distributed Auto Encoder-Gated Recurrent Unit Model," *Sensors 2024*, no. 15, pp. 15-48, 2024, doi: 10.3390/s24154815.

[5] H. Arslantas and S. Okdem, "Indoor Localization With an Autoencoder-Based Convolutional Neural Network," *IEEE Access*, vol. 12, pp. 46059–46066, 2024, doi: 10.1109/access.2024.3382135.

[6] D. Kim, J.-H. Park, and Y.-J. Suh, "Wi-Fi Fingerprinting Indoor Localization Framework Using Feature-Level Augmentation via Variational Graph Auto-Encoder," *Electronics 2025*, vol. 14, p. 2807, 2025, doi: 10.3390/electronics14142807.

[7] J. Zhang and Y. Su, "A Deep Neural Network Based on Stacked Auto-encoder and Dataset Stratification in Indoor Location," *Springer-Verlag*, vol. 14, pp. 33–46, 2021, doi: 10.1007/978-3-030-77964-1_3.

[8] N. Paulson Eberechukwu, H. Park, C. Laoudias, S. Horsmanheimo, and S. Kim, "Dropout Autoencoder Fingerprint Augmentation for Enhanced Wi-Fi FTM-RSS Indoor Localization," *IEEE Communications Letters*, vol. 27, no. 7, pp. 1759-1763, 2023, doi: 10.1109/LCOMM.2023.3272972.

[9] S. Shang and L. Wang, "A robust WiFi localization algorithm using data augmentation and stacked denoising autoencoder," in *Proceedings of the 35th Chinese Control and Decision Conference (CCDC)*, 2023, pp. 1445-1450, doi: 10.1109/CCDC.2023.101745.

[10] M. Nowicki and J. Wietrzykowski, "Low-effort place recognition with Wi-Fi fingerprints using deep learning," *Innovations in Automation, Robotics and Measurement Techniques* 2017.

[11] A. Moreira, M. J. Nicolau, F. Meneses, and A. Costa, "Wi-Fi fingerprinting in the real world - rtls at the evaal competition," in *International Conference on Indoor Positioning and Indoor Navigation (IPIN)*, 2015.

[12] K. S. Kim, R. Wang, Z. Zhong, Z. Tan, H. Song, and J. Cha, "Large-scale location-aware services in access: Hierarchical building/floor classification and location estimation using Wi-Fi fingerprinting based on deep neural networks," in *International Workshop on Fiber Optics in Access Network (FOAN)*, 2017.

[13] K. Kim, S. Lee, and K. Huang, "A scalable deep neural network architecture for multi-building and multi-floor indoor localization based on Wi-Fi fingerprinting," *Big Data Analytics*, vol. 3, no. 1, 2018.

[14] A. Kargar-Barzi, E. Farahmand, N. Taheri Chatrudi, A. Mahani, and M. Shafique, "An Edge-Based WiFi Fingerprinting Indoor Localization Using Convolutional Neural Network and Convolutional Auto-Encoder," *IEEE Access*, vol. 12, pp. 85050-85060, 2024, doi: 10.1109/ACCESS.2024.3412676.

[15] J. Bai, Y. Sun, W. Meng, and C. Li, "Wi-Fi Fingerprint-Based Indoor Mobile User Localization Using Deep Learning," *Wireless Communications and Mobile Computing*, pp. 1-12, 2021, doi: 10.1155/2021/6660990.

[16] W. Qian, F. Lauri, and F. Gechter, "Supervised and semi-supervised deep probabilistic models for indoor positioning problems," *Neurocomputing*, vol. 435, pp. 228-238, 2021, doi: 10.1016/j.neucom.2020.12.131.

[17] Z. Ezzati Khatab, A. Hajihoseini Gazestani, S. A. Ghorashi, and M. Ghavami, "A fingerprint technique for indoor localization using autoencoder based semi-supervised deep extreme learning machine," *Signal Processing*, vol. 181, p. 107915, 2021, doi: 10.1016/j.sigpro.2020.107915.

[18] K. Kim and J. Lee, "Adaptive Scheme of Denoising Autoencoder for Estimating Indoor Localization Based on RSSI Analytics in BLE Environment," *Sensors*, vol. 23, no. 12, p. Art. no. 5544, 2023.

[19] Z. Turgut and A. Gorgulu Kakisim, "An explainable hybrid deep learning architecture for WiFi-based indoor localization in Internet of Things environment," *Future Generation Computer Systems*, vol. 138, 2024, doi: 10.1016/j.future.2023.10.003.

[20] S. Amini and S. Ghaemmaghami, "Sparse Autoencoders Using Non-smooth Regularization," presented at the 2018 26th European Signal Processing Conference (EUSIPCO), Rome, Italy, 2018.

[21] S. Amini, M. Soltanian, M. Sadeghi, and S. Ghaemmaghami, "Non-Smooth Regularization: Improvement to Learning Framework Through Extrapolation," *IEEE Transactions on Signal Processing*, vol. 70, pp. 1213-1223, 2022, doi: 10.1109/TSP.2022.3154969.

[22] X. Kang, X. Liang, and Q. Liang, "Indoor Localization Algorithm Based on a High-Order Graph Neural Network," *Sensors*, vol. 23, no. 19, p. 8221, 2023, doi: 10.3390/s23198221.

[23] D. Kim, J.-H. Park, and Y.-J. Suh, "A Wi-Fi Fingerprinting Indoor Localization Framework Using Feature-Level Augmentation via Variational Graph Auto-Encoder," *Electronics* vol. 14, no. 1114, p. 2807, 2025, doi: 10.3390/electronics14142807.

[24] H. Rizk and A. Elmogy, "SelfLoc: Robust Self-Supervised Indoor Localization with IEEE 802.11az Wi-Fi for Smart Environments," *Electronics*, vol. 14, no. 13, p. 2675, 2025, doi: 10.3390/electronics14132675.

[25] G. Shen, Y. Sun, F. Lu, and a. others, "Enhancing Wi-Fi RSS-Based Indoor Positioning Under Dynamic AP Availability: Leveraging Virtual Feature Maps and Contrastive Learning," *IEEE Sensors Journal*, vol. 13, no. 11, 2024, doi: 10.1109/JSEN.2024.3432585.

[26] N. Salahian, F. A. Tab, S. A. Seyedi, and J. Chavoshinejad, "Deep autoencoder-like NMF with contrastive regularization and feature relationship preservation," *Expert Systems with Applications*, vol. 214, p. 119051, 2023, doi: 10.1016/j.eswa.2022.11905.

[27] N. B. Erichson, Z. Manohar, and S. L. Brunton, "Noise-Injected Autoencoders for Robust Representation Learning," *IEEE Transactions on Neural Networks and Learning Systems*, vol. 31, no. 12, pp. 5537–5548, 2020, doi: doi:10.1109/TNNLS.2020.2992495.

[28] Y. Song, H. Liu, and Q. Chen, "Latent Space Regularization Techniques for Enhanced Autoencoder Generalization," *IEEE Access*, vol. 11, pp. 35621–35633, 2023, doi: 10.1109/ACCESS.2023.3275432.

[29] A. Duque, S. Morin, G. Wolf, and K. R. Moon, "Geometry Regularized Autoencoders," *IEEE Transactions on Pattern Analysis and Machine Intelligence*, vol. 45, no. 6, pp. 7381–7394, 2023, doi: 10.1109/TPAMI.2022.3222104.

[30] H. Steck and D. Garcia Garcia, "On the Regularization of Autoencoders," *arXiv*, p. 2110.11402, 2021, doi: 10.48550/arXiv.2110.11402.

[31] S. Amini and S. Ghaemmaghami, "A new framework to train autoencoders through non-smooth regularization," *IEEE Transactions on Signal Processing*, vol. 67, no. 7, pp. 1860-1874, 2019, doi: 10.1109/TSP.2019.2899294.

[32] A. Lewkowycz and G. Gur-Ari, "On the training dynamics of deep networks with L_2 regularization," *Advances in Neural Information Processing Systems*, vol. 33, pp. 10447–10460, 2020, doi: 10.5555/3495724.3496126.

[33] Z. Liu, Y. Cui, and A. B. Chan, "Improve Generalization and Robustness of Neural Networks via Weight Scale Shifting Invariant Regularizations," *arXiv:2008.02965*, 2020, doi: 10.48550/arXiv.2008.02965.

[34] N. Egwu, T. Mrziglod, and A. Schuppert, "Neural network input feature selection using structured L_2-norm penalization," *Applied Intelligence*, vol. 53, pp. 5732–5749, 2023, doi: 10.1007/s10489-022-03539-8.

[35] Y. Dar, V. Muthukumar, and R. G. Baraniuk, "A farewell to the bias-variance tradeoff, an overview of the theory of overparameterized machine learning," *arXiv*, p. 2109.02355, 2021, doi: 10.48550/arXiv.2109.02355.

[36] M. Belkin, D. Hsu, S. Ma, and S. Mandal, "Reconciling modern machine-learning practice and the classical bias--variance trade-off," *Proceedings of the National Academy of Sciences*, vol. 116, no. 32, pp. 15849-15854, 2019, doi: 10.1073/pnas.1903070116.

[37] S. Wright and J. Nocedal, "Numerical optimization," *Springer Science*, vol. 35, pp. 67–68, 1999.

[38] P. Neal, C. Eric, P. Borja, and E. Jonathan, "Distributed optimization and statistical learning via the alternating direction method of multipliers," *Foundations and Trends in Machine learning*, vol. 3, no. 1, pp. 1-122, 2011.

[39] M. Abadi *et al.*, "Tensorflow: Large-scale machine learning on heterogeneous distributed systems," *arXiv*, 2016, doi: 10.48550/arXiv.1603.04467.

[40] R. Torres-Sospedra *et al.*, "UJIIndoorLoc: A New Multi-building and Multi-floor Database for WLAN Fingerprint-based Indoor Localization Problems," presented at the Proceedings of the Fifth International Conference on Indoor Positioning and Indoor Navigation (IPIN 2014), Busan (Korea), 2014.

[41] X. Zhu, T. Qiu, W. Qu, X. Zhou, M. Atiquzzaman, and D. Wu, "BLS-Location: A Wireless Fingerprint Localization Algorithm Based on Broad Learning," *IEEE Transactions on Mobile Computing*, vol. 22, no. 1, pp. 115-128, 2023, doi: 10.1109/TMC.2021.3073005.

[42] M. Youssef and A. K. Agrawala, "The horus wlan location determination system," presented at the Proceedings of the 3rd International Conference on Mobile Systems, Applications, and Services, ser. MobiSys '05. ACM, 2005.

[43] M. Abbas, M. Elhamshary, H. Rizk, M. Torki, and M. Youssef, "WiDeep: WiFi-based accurate and robust indoor localization system," presented at the IEEE International Conference on Pervasive, 2019.